RESEARCH ARTICLE

WILEY

Relation between palm and finger cortical representations in primary somatosensory cortex: A 7T fMRI study

Michel Akselrod[1,2,3] ⓘ | Roberto Martuzzi[2,4] | Wietske van der Zwaag[5] | Olaf Blanke[2,6] | Andrea Serino[1,2]

[1]Laboratory MySpace, Department of Clinical Neuroscience, University Hospital of Lausanne (CHUV), Lausanne, Switzerland

[2]Laboratory of Cognitive Neuroscience, Brain Mind Institute and Center for Neuroprosthetics, Swiss Federal Institute of Technology of Lausanne (EPFL), Geneva, Switzerland

[3]Minded Program, CMON Unit, Italian Institute of Technology, Genoa, Italy

[4]Foundation Campus Biotech Geneva, Geneva, Switzerland

[5]Spinoza Centre for Neuroimaging, Amsterdam, Netherlands

[6]Department of Neurology, University Hospital, Geneva, Switzerland

Correspondence
Michel Akselrod, Laboratory MySpace, Department of Clinical Neuroscience, University Hospital of Lausanne (CHUV), Avenue Beaumont, Pavillon 4, CH-1011 Lausanne, Switzerland.
Email: michel.akselrod@gmail.com

Olaf Blanke, Laboratory of Cognitive Neuroscience, Center for Neuroprosthetics, Ecole Polytechnique Fédérale de Lausanne (EPFL), Campus Biotech H4, Pavillon 4 Chemin des Mines 9, CH-1202 Geneva, Switzerland.
Email: olaf.blanke@epfl.ch

Abstract

Many studies focused on the cortical representations of fingers, while the palm is relatively neglected despite its importance for hand function. Here, we investigated palm representation (PR) and its relationship with finger representations (FRs) in primary somatosensory cortex (S1). Few studies in humans suggested that PR is located medially with respect to FRs in S1, yet to date, no study directly quantified the somatotopic organization of PR and the five FRs. Importantly, the link between the somatotopic organization of PR and FRs and their activation properties remains largely unexplored. Using 7T fMRI, we mapped PR and the five FRs at the single subject level. First, we analyzed the cortical distance between PR and FRs to determine their somatotopic organization. Results show that PR was located medially with respect to D5. Second, we tested whether the observed cortical distances would predict the relationship between PR and FRs activations. Using three complementary measures (cross-activations, pattern similarity and resting-state connectivity), we show that the relationship between PR and FRs activations were not determined by their somatotopic organization, that is, there was no gradient moving from D5 to D1, except for resting-state connectivity, which was predicted by the somatotopy. Instead, we show that the representational geometry of PR and FRs activations reflected the physical structure of the hand. Collectively, our findings suggest that the spatial proximity between topographically organized neuronal populations do not necessarily predicts their functional properties, rather the structure of the sensory space (e.g., the hand shape) better describes the observed results.

KEYWORDS
7T fMRI, palm and finger cortical representations, primary somatosensory cortex

Olaf Blanke and Andrea Serino contributed equally to this work.

1 | INTRODUCTION

The sensory cortices of the mammalian brain are topographically organized to form structured maps of the represented sensory features. This organizational principle is preserved across species, sensory modalities, and individuals (Kaas, 1997; Udin & Fawcett, 1988) and the role of this topographic organization and its relevance for shaping functional brain responses are important topics for fundamental and clinical research. Due to metabolic and structural constraints, the spatial proximity between topographically organized neuronal populations directly impacts their functional coupling (i.e., spatially close neurons are more likely to form synapses than distant ones) (van Ooyen et al., 2014; van Pelt & van Ooyen, 2013). On the other hand, the statistics of natural stimulation received during everyday life drives the tuning of functional neuronal responses through activity-dependent plasticity and can reinforce the functional coupling between distant neuronal populations (Buonomano & Merzenich, 1998). The somatosensory system is a particularly relevant model to study the relationship between topographic organization in neural maps, properties of functional brain responses and use-related function. The somatosensory system represents elements (i.e., body parts) that can move with respect to each other (e.g., the configuration of the five fingers during object manipulation), can directly interact with each other (i.e., self-touch) and need to fulfill many different sensorimotor functions. While the somatosensory representations of fingers have been researched extensively, the palm has been less studied despite its importance for hand function and despite being anatomically connected with all five fingers. The aim of the present study is to investigate the topographical and functional organization of tactile representation of the palm (palm representation, PR) and its relationship with the tactile representations of the five fingers (fingers representations, FRs) in the human primary somatosensory cortex, S1.

S1 is somatotopically organized into a cortical map of the contralateral half of the body (Kaas, Nelson, Sur, Lin, & Merzenich, 1979; Rasmussen & Penfield, 1947). FRs in S1 appear in a latero-medial sequence (D1—D2—D3—D4—D5). This organization is consistent across individuals as shown in recent ultra-high field (7T) fMRI studies (Besle, Sánchez-Panchuelo, Bowtell, Francis, & Schluppeck, 2014; Martuzzi, van der Zwaag, Farthouat, Gruetter, & Blanke, 2014; Sanchez-Panchuelo et al., 2012, 2014; Sanchez-Panchuelo, Francis, Bowtell, & Schluppeck, 2010; Schweisfurth, Frahm, Farina, & Schweizer, 2018; Schweisfurth, Frahm, & Schweizer, 2014; Schweisfurth, Schweizer, & Frahm, 2011; Schweizer, Voit, & Frahm, 2008; Stringer et al., 2014; Stringer, Chen, Friedman, Gatenby, & Gore, 2011). While the S1 representations of the base of the fingers (i.e., the distal part of the palm) with respect to FRs have been described in a consistent manner (Blankenburg, Ruben, Meyer, Schwiemann, & Villringer, 2003; Sanchez-Panchuelo et al., 2012, 2014; Schweisfurth et al., 2011, 2014), reports concerning the S1 representations of the proximal part of the palm, which is the focus of the present study, are mixed. Several studies suggested that PR is located medially with respect to FRs in S1 (Blankenburg et al., 2003; Moore et al., 2000; Rasmussen & Penfield, 1947). However, other

studies, specifically aiming at mapping FRs and PR, failed to detect a clear PR and could not determine the palm to finger sequence in human S1, likely because they used neuroimaging without sufficient spatial resolution (MEG) or tactile stimulation protocols non-optimized for mapping PR (Hashimoto, Mashiko, Kimura, & Imada, 1999; Sanchez-Panchuelo et al., 2012). Importantly, none of these studies provided direct quantification of the somatotopic organization of the five fingers and the palm.

The present study aimed at mapping bilateral PR and FRs in S1 at the level of single subjects and investigates the relationship between somatotopic and functional organizations. To this aim, we applied a 7T fMRI mapping procedure that was validated in previous studies (Akselrod et al., 2017; Martuzzi et al., 2014, 2015; Mehring et al., 2019; Serino et al., 2017). First, we analyzed the cortical distance between PR and the five FRs to determine the somatotopic sequence in S1. This was done in order to validate the proposed serial somatotopic arrangement D1—D2—D3—D4—D5—PALM. Second, in order to evaluate the relationship between somatotopic and functional organizations, we tested to which extent the activation properties of PR and FRs matched their somatotopic organization. We performed the following analyses to quantify the activation properties of PR and FRs: (a) we measured the degree of cross-activation between PR and FRs during tactile stimulation of the palm and of the fingers; (b) we compared the multi-voxel patterns of activity in S1 during tactile stimulation of the palm and of the fingers; (c) we quantified the resting-state functional connectivity between PR and FRs.

Based on previous reports in humans (Blankenburg et al., 2003; Moore et al., 2000; Rasmussen & Penfield, 1947), we predicted that PR would be located medially with respect to D5 corresponding to a serial somatotopic arrangement. It is possible that the somatotopic arrangement of PR and FRs affects their activation properties (i.e., more comparable activations between closer representations); if this was the case, a serial somatotopic arrangement would predict that activation properties should be most comparable between PALM-D5 representations, with a further decreasing gradient from D4 to D1 and the weakest association between PALM-D1 representations. However, considering that the palm is often recruited concomitantly with the five fingers during most in-hand manipulation activities (Bullock & Dollar, 2011; Pont, Wallen, & Bundy, 2009) and that the similarity between hand representations reflect the natural usage of hands (Ejaz, Hamada, & Diedrichsen, 2015), we hypothesize that the activation properties of PR and FRs should not match a potential serial somatotopic arrangement (i.e., the palm would not be coupled preferentially with D5, then D4, D3, …). To provide further insights into the relationship between hand somatotopic organization and hand activation properties, we compared the representational geometry of the aforementioned measures (i.e., cortical distances, cross-activations, multi-voxel activity patterns and functional connectivity) with various competitive models: two models based on the physical structure of the hand ("Body model" and "Perceived body model") and two purely conceptual models based on different possible configurations of palm and fingers ("Linear model" and "Circular model").

2 | METHODS

2.1 | Subjects

Fifteen healthy subjects (five females) aged between 18 and 39 years old (mean ± SD: 24.3 ± 5.2 years) participated in the study. One participant was excluded due to excessive head motion during MRI acquisition (up to 5 mm of movement in the z-direction).

Data from another group of nine healthy subjects (five females, aged between 26 and 33 years old) recruited in a previous study (Mehring et al., 2019) was used to extract average hand dimensions (see Section 2.11).

All participants were right-handed as assessed orally using the Edinburgh Handedness Inventory (Oldfield, 1971).

All subjects gave written informed consent, all procedures were approved by the Ethics Committee of the Faculty of Biology and Medicine of the University of Lausanne, and the study was conducted in accordance with the Declaration of Helsinki.

2.2 | Experimental procedure

During fMRI acquisition, subjects received tactile stimulation on six skin regions on both hands (D1—D2—D3—D4—D5—PALM). Tactile stimulation was delivered on the palmar side and consisted of a gentle manual stroking at a rate of approximately 1 Hz performed by an experimenter with his index finger, who received instructions by means of MR compatible earphones. To reduce the variability of the tactile stimulation across participants and to guarantee that a reliable and constant pressure was exerted, the stroking was always performed by the same experimenter, who received extensive training prior to data acquisition. As shown in previous studies, natural touch induces very reliable BOLD signal responses in S1 and is well suited to study body representations in S1 (Akselrod et al., 2017; Martuzzi et al., 2014, 2015; Serino et al., 2017; Van Der Zwaag, Gruetter, & Martuzzi, 2015). The participant's fingers were repeatedly stroked on the palmar side of the two distal phalanges (thus preventing contamination with palm stimulation). The participant's palms were stroked on the palmar side and along a vertical strip of skin located in the center of the palm and of comparable size with respect to finger stimulation (Figure 1). One fMRI run for each hand was acquired in pseudo-randomized order across participants. Within each run, the six regions of the same hand were stroked in a fixed order using a block design (D1—D3—D5—D2—D4—PALM) and each hand region was stimulated during four blocks. Each stimulation block included 20 strokes delivered at 1 Hz on the same hand region. Each block lasted 20 s and was followed by a rest period of 10 s (i.e., rest periods with no tactile stimulation) with a total of 24 blocks. In addition to tactile stimulation runs, resting-state data (5 min, eyes closed) and anatomical images were acquired for each participant.

2.3 | Data acquisition

MR images were acquired using a short-bore head-only 7 Tesla scanner (Siemens Medical, Germany) equipped with a 32-channel Tx/Rx RF-coil
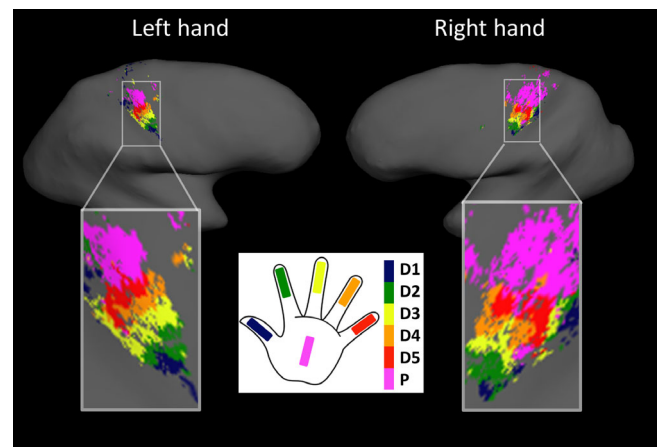

FIGURE 1 Palm to fingers somatotopy. S1 hand map of a representative subject suggesting the following arrangement in humans: D1—D2—D3—D4—D5—PALM

(Nova Medical; Salomon, Darulova, Narsude, & Van Der Zwaag, 2014). Functional images were acquired using a sinusoidal readout EPI sequence (Speck, Stadler, & Zaitsev, 2008) and comprised of 28 axial slices placed approximately orthogonal to the postcentral gyrus (voxel resolution = $1.3 \times 1.3 \times 1.3$ mm^3, TR = 2 s, TE = 27 ms, flip angle = 75°, matrix size = 160x160, FOV = 210 mm, GRAPPA factor = 2). The mapping sequence included 361 volumes for each run and the resting-state sequence included 150 volumes. For the resting-state sequence, cardiac and respiratory signals were acquired. Anatomical images were acquired using an MP2RAGE sequence (Marques et al., 2010, resolution = $1 \times 1 \times 1$ mm^3, TE = 2.63 ms, TR = 7.2 ms, TI1 = 0.9 s, TI2 = 3.2 s, TR_{mprage} = 5 s). To aid co-registration between the functional and the anatomical images, a whole brain EPI volume was also acquired with the same inclination used in the functional runs (81 slices, resolution = $1.3 \times 1.3 \times 1.3$ mm^3, TR = 5 s, TE = 27 ms, flip angle = 75°, matrix size = 160×160, FOV = 210 mm, GRAPPA factor = 2).

2.4 | Data preprocessing

All images were preprocessed using the SPM8 software (Wellcome Department of Cognitive Neurology, London, UK). Preprocessing of fMRI data included slice timing correction, spatial realignment, and minimal smoothing (FWHM = 2 mm). Freesurfer (http://surfer.nmr.mgh.harvard.edu/, version 6) was used for surface reconstruction (recon-all), for computing cortical distance along the surface (see Section 2.6) and for surface rendering of S1 hand maps of a representative subject (Figure 1c). The MRIcron software was used for visualizing results in 3D space for all subjects (McCausland Center for Brain Imaging, University of South Carolina, United States, http://www.mccauslandcenter.sc.edu/mricro/mricron). The Connectome Mapper 3 software was used for anatomical parcellation of each subject's mp2rage data with respect to gyral and sulcal structure in native space (Tourbier, Aleman-Gomez, Griffa, Bach Cuadra, & Hagmann, 2020), which is based on the Desikan-Killiany parcellation (FreeSurfer 6, Desikan et al., 2006).

2.5 | Definition of somatosensory hand representations

Independently for each subject and each hand, the clusters corresponding to the representations of each stimulated hand region were delimited using an automated approach validated in previous publications (Akselrod et al., 2017; Martuzzi et al., 2014, 2015; Serino et al., 2017). A GLM analysis (SPM8) was carried out to estimate the response induced by the stimulation of the different hand regions. The model included six regressors (one for each stimulated hand region) convolved with the hemodynamic response and the corresponding first-order time derivatives, as well as the six rigid-body motion parameters as nuisance regressors. The zero-order main regressors were used for subsequent statistical inferences. For each hand separately, an F-contrast ($p < .0001$ uncorrected) across all stimulated hand regions was computed. The active voxels within the F-contrast were used as a functional S1 mask to identify all voxels responding to at least the stimulation of one hand region. T-contrasts (against rest) were also computed for each stimulated hand region. Finally, for each subject separately, an anatomical parcellation of left and right S1 in native space (i.e., anatomical S1 mask) was computed (Connectome Mapper 3). Then, based on a "winner takes all" approach, each voxel contained within the anatomical and functional S1 masks was labeled as representing the hand region whose stimulation elicited the highest t-score (against rest) for that particular voxel. This approach produces continuous and non-overlapping S1 maps comparable to phase encoding approaches used in mapping studies (Olman et al., 2010; Saadon-Grosman, Tal, Itshayek, Amedi, & Arzy, 2015; Sanchez-Panchuelo et al., 2012; Zeharia, Hertz, Flash, & Amedi, 2015).

2.6 | Analysis of cortical distances

Within each identified hand region representation, the coordinates of the peak activation (maximum t-value) were extracted. These 3D coordinates were transformed into indices of the nearest vertices on the surface space. The surface distances (geodesic) between PR and FRs were calculated for each participant using FreeSurfer (mris_pmake). The statistical analysis described below (Section 2.10) was conducted to assess whether the cortical distance was increasing between PR and FRs as expected by a serial somatotopic arrangement: "PALM-D1 > PALM-D2 > PALM-D3 > PALM-D4 > PALM-D5".

2.7 | Analysis of cross-activations

To investigate the activation properties of PR and FRs, we computed the cross-activations between PR and FRs. To this end, we computed the average BOLD response (beta values) within each FR during the stimulation of the palm (P -> FR), as well as the average BOLD response within PR during the stimulation of each finger (F -> PR). The computed average BOLD responses were normalized with respect to the maximum response observed in each hand representation (i.e., by definition the response to stimulation of the represented hand region). Cross-activations between PR and each FR were defined as the average between P -> FR and F -> PR. This analysis was conducted in the native space of individual subjects. The statistical analysis described below (Section 2.10) was conducted to assess whether cross-activations between PR and FRs reflected their somatotopic arrangement.

2.8 | Analysis of multi-voxel activity patterns

To further investigate the activation properties of PR and FRs, we compared the multi-voxel activity patterns associated with palm and fingers stimulation (Kriegeskorte, Mur, & Bandettini, 2008). Compared to the analysis of cross-activations, this measure does not rely on the definition of hand region representations associated with each body part stimulated. Separately for each participant and each hand, we computed a GLM analysis to estimate the beta parameters associated with each period of tactile stimulation (24 tactile stimulation regressors and 6 rigid body motion regressors). Within the active voxels identified to define somatosensory hand representations (see Section 2.5), the cross-validated (odd-even split across trials) Mahalanobis distance (Nili et al., 2014) between activity patterns associated with palm and fingers stimulation was computed as a measure of pattern dissimilarity. For each activity pattern, the mean activity across voxels was subtracted. This analysis was conducted in the native space of individual subjects. The statistical analysis described below (Section 2.10) was conducted to assess whether the multi-voxel activity patterns associated with palm and fingers stimulation reflected the somatotopic arrangement of PR and FRs.

2.9 | Analysis of resting-state functional connectivity

Compared to the analyses of cross-activations and multi-voxel activity patterns, this measure quantifies the activation properties of PR and FRs in the absence of tactile stimulation. Resting-state data were processed using the Conn toolbox (Whitfield-Gabrieli & Nieto-Castanon, 2012). At each voxel, the BOLD signal was band-pass filtered (0.008–0.09 Hz). The cardiac and respiratory related components of the BOLD signal were estimated using the RETROICOR algorithm (Glover, Li, & Ress, 2000) and regressed out from the data. The average BOLD signal of white matter and cerebrospinal fluid and the six estimated motion parameters were also included as nuisance regressors in the model. The bivariate temporal correlations between PR and FRs were calculated from the preprocessed BOLD time-courses of the resting state run. The obtained correlation coefficients were transformed into z-values by applying the Fisher transform (Fisher, 1915). This analysis was conducted in the native space of individual subjects. The statistical analysis described below (Section 2.10) was conducted to assess whether rs-FC between PR and FRs reflected their somatotopic arrangement.

2.10 | Statistical hypotheses and analyses

First, we used Bayesian statistics to investigate the relationship between PR and FRs across fingers and across body side using the data obtained from the analyses of cortical distances, of cross-activations, of multi-voxel activity patterns and of resting-state functional connectivity. Separately for each measure, we computed a two-way Bayesian repeated-measures ANOVA with "FINGER" (five levels: P-D1, P-D2, P-D3, P-D4, and P-D5) and "SIDE" (two levels: right hand, RH, and left hand, LH) as within-subject factors (JASP v0.13). Main effects associated with the factor of "FINGERS" were not further investigated using pair-wise comparisons as we designed specific *hypothesis driven* tests to investigate the relationship between the different levels of this factor (see below).

Second, we aimed at validating specific hypotheses regarding the somatotopic and functional organization of hand representations. In particular, we directly tested the hypothesis that PR and FRs are organized in serial arrangement in human S1 (see serial arrangement in Figure 1a, Moore et al., 2000; Rasmussen & Penfield, 1947). In addition, we speculated that such organization would not be reflected in the activation properties of PR and FRs as PR would not be coupled preferentially with D5, then with D4, then with D3, then with D2 and least with D1 (Bullock & Dollar, 2011; Pont et al., 2009). To test these hypotheses, we used the R package *bain* (Hoijtink, Mulder, Lissa, & Gu, 2019), which allows computing Bayesian statistics based on *informative* hypotheses (i.e., *hypothesis driven* tests). We computed Bayesian one-way repeated-measures ANOVAs separately for each measure (cortical distance, cross-activations, multi-voxel activity patterns and resting-state functional connectivity) and each body side (right hand and left hand). We compared three hypotheses: (1) H_1, a hypothesis of equivalence between the tested variables with a difference between pairs of variables smaller than a Cohen's *d* of 0.2 (P-D1 ≈ P-D2 ≈ P-D3 ≈ P-D4 ≈ P-D5) (Sawilowsky, 2009), (2) H_2, a hypothesis of ordering between the tested variables (P-D1 > P-D2 > P-D3 > P-D4 > P-D5 for cortical distance and pattern dissimilarity or P-D1 < P-D2 < P-D3 < P-D4 < P-D5 for cross-activations and functional connectivity), (3) and H_u (P-D1, P-D2, P-D3, P-D4, P-D5), the alternative unrestricted hypothesis (i.e., the null hypothesis).

Finally, we computed a Bayesian regression between each functional measure as observed variable (cross-activations, multi-voxel activity patterns and resting-state functional connectivity) and cortical distance as predictor variable (JASP v0.13).

For each Bayesian test, we assumed equal prior probabilities and report the Bayes factors (BF) and posterior probabilities (PP). We considered Bayesian factors >3 as positive evidence, >10 as strong evidence, >30 as very strong evidence (Kass & Raftery, 1995).

2.11 | Dissimilarity analysis

To further investigate the functional organization of hand representations, we conducted dissimilarity analysis (Akselrod et al., 2017; Kriegeskorte et al., 2008) and compared the representational geometry associated with the computed measures (cortical distances, cross-activations, multi-voxel activity patterns, and functional connectivity) with three models of hand representation. Separately for each subject and each hand, the four measures of dissimilarity (cortical distances, cross-activations, multi-voxel activity patterns and functional connectivity) were computed between all pairs of fingers in addition to between each finger and the palm to form a 6x6 dissimilarity matrix. The computed dissimilarity matrices were compared with: (a) a model based on the physical shape of the hand, termed "Body" model; (b) a model of somatotopy reflecting the serial arrangements of FRs and PR, termed "Linear" model; (c) a control model, termed "Circular" model.

The "cortical distance" dissimilarity was computed as the surface distance between the coordinates of peak activations associated with the stimulated hand regions similarly to the analysis presented in Section 2.6.

The "cross-activation" dissimilarity was computed as the cross-activations between pairs of S1 hand representations similarly to the analysis presented in Section 2.7. The cross-activations between pairs of S1 hand representations correspond to a measure of similarity, that is, pairs of S1 hand representations are considered similar if they are reciprocally cross-activated when stimulated separately. The 6x6 similarity matrices of cross-activations were transformed into 6x6 dissimilarity matrices by subtracting each cross-activation from 1 (i.e., 1 - cross-activation), where 1 corresponds to the maximum response (see Section 2.7).

The "multi-voxel activity pattern" dissimilarity was computed as the cross-validated mahalanobis distance between the multi-voxel patterns of S1 activations associated with the stimulated hand regions similarly to the analysis presented in Section 2.8.

The "functional connectivity" dissimilarity was computed based on the resting-state functional connectivity between pairs of S1 hand representations similarly to the analysis presented in Section 2.9. The resting-state functional connectivity is a measure of similarity, and it was transformed into a measure of dissimilarity by subtracting the bivariate correlation to 1 (i.e., 1-correlation).

The "Body" model was computed using an independent dataset including nine healthy controls from a previous study (Mehring et al., 2019). The data consisted in the location of different parts on the back of their right hand including the tip and second knuckle of each finger, as well as the center of the hand (i.e., the palm). Using these data, we computed average pair-wise distances between the fingers (defined as the average location between the tip and the second knuckle) and the center of the palm. This resulted in a single "Body" model (Figure 6a). The "Linear" model was conceived as a regular decrease in similarity between each adjacent element of the matrix with a step of 1 (arbitrary unit), we note that this model corresponds to a serial model of S1 somatotopy with perfect spacing between representations (Figure 6b). The "Circular model" was conceived as a control model reflecting a plausible geometry of hand representations, but not related to the body or to S1 somatotopy with the palm located in the center and the fingers arranged radially around the palm (Figure 6c).

The matrices corresponding to the four measures of dissimilarity were correlated with the matrices corresponding to the three models

separately for each participant (upper part of the matrices was treated as data vectors). For each measure, an upper bound limit of maximum correlation (i.e., noise ceiling) was calculated and graphically displayed. The theoretical best model that could be fitted to the data corresponds to the average dissimilarity matrix across subjects (Ejaz et al., 2015). As such, separately for each measure, the noise ceiling was computed as the correlation between each subject's dissimilarity matrix and the group average dissimilarity matrix, averaged across subjects. In order to compare the different models, the resulting correlation values were normalized using the Fischer transformation and statistically analyzed using Bayesian paired t-tests between the model with the highest correlation and the other two models (JASP v0.13). We considered Bayesian factors >3 as positive evidence, >10 as strong evidence, >30 as very strong evidence (Kass & Raftery, 1995).

For display purposes, we used classical multidimensional scaling (also known as Principal Coordinate Analysis, Cooper & Seber, 1985) to represent the models and the dissimilarity measures on a 2D plot.

2.12 | Data and code availability statement

The final data presented in Section 3 (cortical distances, cross-activations, multi-voxel patterns, resting-state functional connectivity, and dissimilarity analysis) are openly available on the Zenodo platform. Data analyses were carried out using publicly available resources and/or are fully reproducible from the information provided in Section 2. Raw data will not be shared to guarantee privacy and confidentiality for the participants.

3 | RESULTS

Twelve hand regions (six on each hand) were stimulated during fMRI acquisition to map their cortical representations within S1. This led to a total of 12 mapped representations in S1 per subject (see Section 2).

Visual inspection of individual maps suggested that the palm (i.e., PRs) was located medially with respect to the D5 FR in all participants. The S1 hand maps of a representative subject are shown in Figure 1 and S1 hand maps for all subjects are shown in Supporting Information (-Figures S1–S2).

3.1 | Cortical distance

We compared the geodesic distance between PR and each FR using Bayesian statistics (see Section 2.10). As shown in Figure 2, the distance between PR and each FR is decreasing when moving from P-D1 to P-D5.

The two-way ANOVA showed a main effect of finger (BF = $2.011e^{+18}$, PP = 0.866), a main effect of body side (BF = 3,396.92, PP = 0.866), but no interaction (BF = 0.154, PP = 0.134). The main effect of body side, with very strong evidence (BF > 100), was due to reduced distances for left hand representations compared to the right hand.

The *hypothesis driven* ANOVAs strongly supported the ordering hypothesis, H_2, for both hands, suggesting a latero-medial serial arrangement, with the palm located after D5: "D1 - D2 - D3 - D4 - D5 - PALM" (right hand: BF = 25.487, PP = 0.963; left hand: BF = 38.73, PP = 0.975, see Table 1). We note that we replicated the analysis of cortical distances using the centers of mass as landmarks to compute cortical distances and found similar results (Figure S3).

To summarize, the analysis of cortical distances comprehensively suggests a serial latero-medial arrangement, with the palm being represented most laterally in human S1. In addition, we found reduced cortical distances between PR and FRs for left hand representations.

3.2 | Cross-activations

We then analyzed the cross-activations between PR and FRs, which assess how strongly these representations are reciprocally cross-
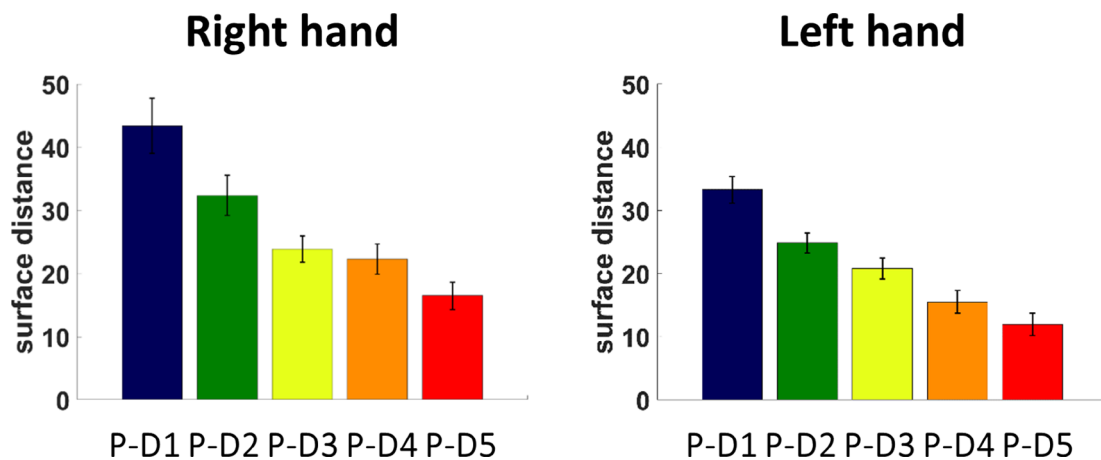

FIGURE 2 Cortical distance. Bar plots of the cortical distances between PR and each FR in the left hemisphere (right hand representations) and in the right hemisphere (left hand representations). Error bars represent the *SEM*

activated when stimulated separately. As shown in Figure 3, there was no consistent evidence of an ordering effect, rather the strongest cross-activations are found between P-D1 and P-D5.

The two-way ANOVA showed a main effect of finger (BF = 33,129.2, PP = 0.976), but no main effect of body side (BF = 0.661, PP = 0.388) and no interaction (BF = 0.063, PP = 0.024).

The *hypothesis driven* ANOVAs supported the unrestricted hypothesis, H_0, for both hands (right hand: PP = 0.863; left hand: PP = 0.997, see Table 2). These results show that cross-activations between PR and FRs do not follow a pattern predicted by the somatotopic organization and do not show equivalent cross-activations between PR and the five FRs. Finally, we did not find evidence for a relationship between cross-activations and cortical distances (BF = 0.395, PP = 0.283).

To summarize, these analyses suggest that cross-activations during isolated stimulation are not equivalent between the PR and each

other FRs, but rather that PR might be preferentially coupled with some FRs, namely D1 and D5. They also do not reflect the somatotopic sequence in S1, suggesting that if a specific pattern of cross-activations between PR and FRs exist, it does not follow the somatotopic organization. These results might suggest the presence of other patterns of cross-activations that were not formulated in our hypotheses, and therefore, to address this point, we performed dissimilarity analysis that is presented below (Section 3.5).

3.3 | Multi-voxel activity patterns

We then compared the dissimilarity (i.e., mahalanobis distance) between multi-voxel activity patterns in S1 associated with the tactile stimulation of the palm and of the five fingers. As shown in Figure 4, the highest dissimilarity was observed between P-D3 for both hands,

TABLE 1 Bayesian statistics on cortical distances

	Right hand		Left hand	
	BF	P(H)	BF	P(H)
H_1 (equivalence): $\mu_1 \approx \mu_2 \approx \mu_3 \approx \mu_4 \approx \mu_5$	0.0	0.0	0.0	0.0
H_2 (ordering): $\mu_1 > \mu_2 > \mu_3 > \mu_4 > \mu_5$	**25.87**	**0.963**	**38.73**	**0.975**
H_u (unrestricted): $\mu_1, \mu_2, \mu_3, \mu_4, \mu_5$		0.037		0.025

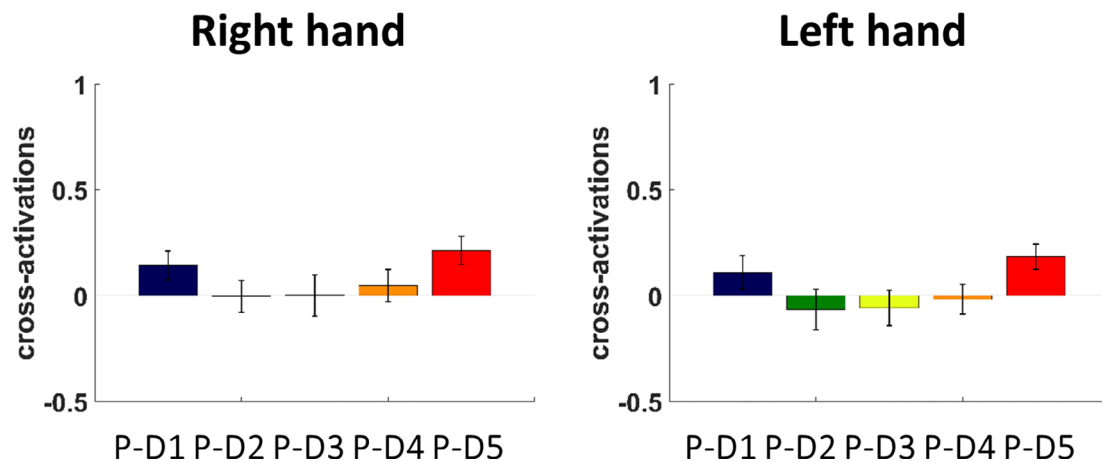*Note:* Hypothesis with highest posterior probability highlighted in bold.

FIGURE 3 Cross-activations. Bar plots of the cross-activations between PR and each FR for the right hand (represented in the left hemisphere) and for the left hand (represented in the right hemisphere). Error bars represent the *SEM*

TABLE 2 Bayesian statistics on cross-activations

	Right hand		Left hand	
	BF	P(H)	BF	P(H)
H_1 (equivalence): $\mu_1 \approx \mu_2 \approx \mu_3 \approx \mu_4 \approx \mu_5$	0.0	0.0	0.0	0.0
H_2 (ordering): $\mu_1 < \mu_2 < \mu_3 < \mu_4 < \mu_5$	0.160	0.138	0.003	0.003
H_u (unrestricted): $\mu_1, \mu_2, \mu_3, \mu_4, \mu_5$		**0.863**		**0.997**

Note: Hypothesis with highest posterior probability highlighted in bold.
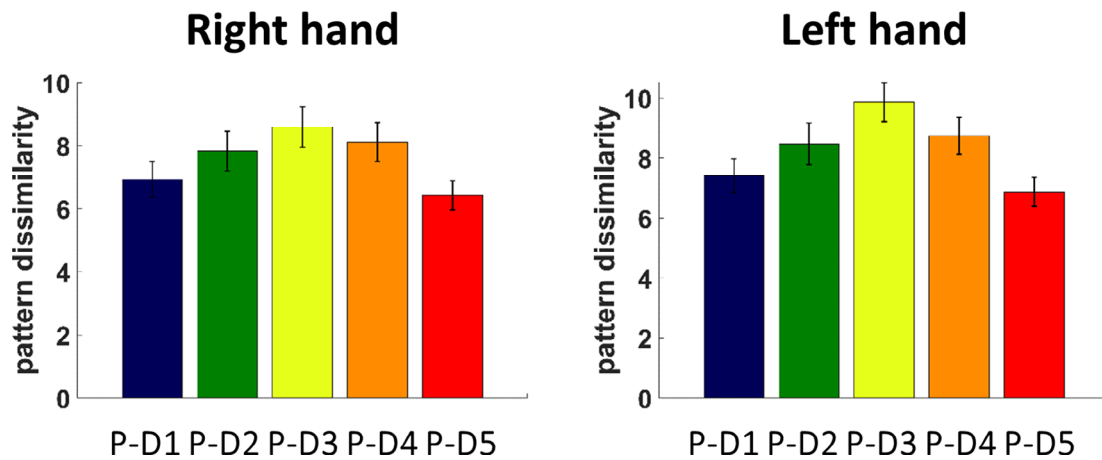
Right hand

Left hand

FIGURE 4 Multi-voxel activity patterns. Bar plots of the dissimilarity between multi-voxel activity patterns associated with the stimulation of the palm and of each finger in the left hemisphere (right hand representations) and in the right hemisphere (left hand representations). Error bars represent the *SEM*

while the lowest dissimilarity was observed between palm-D1 and palm-D5 for both hands. This result is compatible with the cross-activation pattern between PR and FRs (i.e., more coupling between P-D1 and P-D5).

The two-way ANOVA showed a main effect of finger (BF = $1.455e^{+9}$, PP = 0.911), and a main effect of body side (BF = 21.906, PP = 0.871), but no interaction (BF = 0.102, PP = 0.089). The main effect of side was due to increased pattern dissimilarity for the left hand.

The *hypothesis driven* ANOVAs supported the unrestricted hypothesis, H_0, for both hands (right hand: PP = 1.0; left hand: PP = 1.0, see Table 3). These results show that multi-voxel activity patterns do not follow a pattern predicted by the somatotopic organization and do not follow a pattern of equivalence between the palm and the fingers. Finally, we did not find evidence for a relationship between multi-voxel activity patterns and cortical distances (BF = 0.215, PP = 0.177).

To summarize, these analyses suggest that the dissimilarity between multi-voxel activity patterns are not equivalent between the palm and the five fingers and do not reflect the somatotopic sequence in S1. Consistent with the results of the cross-activations analysis (Section 3.2), we observed for both hands that minimal pattern dissimilarity was found between P-D1 and P-D5, possibly suggesting the presence of yet another pattern of functional coupling between PR and FRs that was not formulated in our hypotheses (see dissimilarity analysis, Section 3.5).

3.4 | Resting-state functional connectivity

Finally, we compared the functional connectivity between PR and FRs. As shown in Figure 5, there is a qualitative trend towards stronger functional connections between PR and FRs which are located closer to PR in S1, although this pattern is not fully consistent

TABLE 3 Bayesian statistics on multi-voxel activity patterns

	Right hand		Left hand	
	BF	P(H)	BF	P(H)
H_1 (equivalence): $\mu_1 \approx \mu_2 \approx \mu_3 \approx \mu_4 \approx \mu_5$	0.0	0.0	0.0	0.0
H_2 (ordering): $\mu_1 > \mu_2 > \mu_3 > \mu_4 > \mu_5$	0.0	0.0	0.0	0.0
H_u (unrestricted): $\mu_1, \mu_2, \mu_3, \mu_4, \mu_5$		**1.0**		**1.0**

Note: Hypothesis with highest posterior probability highlighted in bold.

(e.g., P-D1 > P-D2 for the right hand, P-D1 $\approx$ P-D2 and P-D4 $\approx$ P-D5 for the left hand).

The two-way ANOVA showed a main effect of finger (BF = 113.943, PP = 0.914), a main effect of body side (BF = 153.667, PP = 0.916), but no interaction (BF = 0.086, PP = 0.078). The main effect of body side, with very strong evidence (BF > 100), was due to reduced functional connectivity for right hand representations compared to the left hand. We note that this is effect is consistent with the effect of increased cortical distances for right hand representations, which would predict reduced functional connectivity with increased distances.

The *hypothesis driven* ANOVAs supported the ordering hypothesis, H_2, for both hands with positive evidence for the right hand and strong evidence for the left hand (right hand: BF = 1.235, PP = 0.553; left hand: BF = 44.70, PP = 0.978, see Table 4). We note that, for the right hand, low positive evidence was found for the ordering hypothesis, H^2, which can be attributed to stronger functional connectivity for P-D1 compared to P-D2. These results show that the functional connectivity between PR and FRs follows, at least to some extent, a pattern predicted by the somatotopic organization. Finally, we found very strong evidence for a relationship between functional connectivity and cortical distances with stronger functional connectivity being associated with reduced cortical distance (BF = 1,058.725, PP = 0.999).

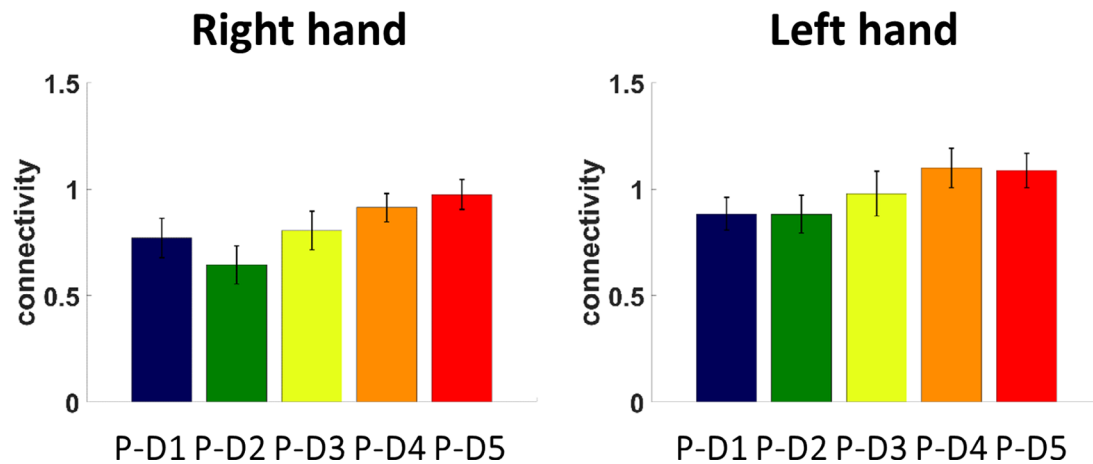## Right hand

Left hand

FIGURE 5 Functional connectivity. Bar plots of the functional connectivity (Z-score) between PR and each of the FR in the left hemisphere (right hand representations) and in the right hemisphere (left hand representations). Error bars represent the *SEM*

TABLE 4 Bayesian statistics on functional connectivity

	Right hand		Left hand	
	BF	P(H)	BF	P(H)
H_1 (equivalence): $\mu_1 \approx \mu_2 \approx \mu_3 \approx \mu_4 \approx \mu_5$	0.0	0.0	0.0	0.0
H_2 (ordering): $\mu_1 < \mu_2 < \mu_3 < \mu_4 < \mu_5$	**1.235**	**0.553**	**44.70**	**0.978**
H_u (unrestricted): $\mu_1, \mu_2, \mu_3, \mu_4, \mu_5$		0.447		0.022

Note: Hypothesis with highest posterior probability highlighted in bold.

To summarize, these functional connectivity results suggest that resting-state functional connectivity between PR and FRs reflect, at least partially, the somatotopic sequence in S1. This is further supported by the strong evidence for a negative relationship between functional connectivity and cortical distance.

3.5 | Dissimilarity analysis

Considering that, with the exception of functional connectivity, the measures of cross-activations and multi-voxel activity patterns were not associated with the somatotopic ordering hypothesis nor with the equivalence hypothesis, we extended previous analyses to investigate the representational geometry of PR and FRs associated with each of the computed measures (cortical distances, cross-activations, multi-voxel activity patterns and functional connectivity). We computed dissimilarity matrices based on these four measures and compared them with three models of hand representation, the "Body" model, the "Linear" model and the "Circular" model. Figure 6 shows the four models (a–c) and the three dissimilarity measures (d–g) with their corresponding 2D configuration computed with multidimensional scaling. We note that in this analysis, similar results were obtained for both hands, thus the data were averaged across both hands. Separate data for right and left hands are shown in Supporting Information (Figures S4–S5).

The three models were designed to capture different aspects of what S1 could represent. The "Body" model formed a 2D

configuration compatible with the shape of a hand. The "Linear" model formed a 2D configuration compatible with the somatotopic sequence "D1-D2-D3-D4-D5-PALM". Finally, the "Circular" model formed a 2D configuration corresponding to a plausible geometry of hand representations, but different from the real shape of a hand and different from S1 hand somatotopic organization.

To assess which model best described the four dissimilarity measures (cortical distances, cross-activations, multi-voxel activity patterns and functional connectivity), we computed the correlation between each dissimilarity matrix and the three models and computed Bayesian paired t-tests across these correlations to identify the best models (Table S1). For cortical distance, we found that the "Linear" model was the best ($r = 0.80 \pm 0.13$) and outperformed the other models with very strong evidence (Linear ≠ Body: BF = 173.96, Linear ≠ Circular: B = 22,670.11). For cross-activations, we found that the "Body" model was the best ($r = 0.80 \pm 0.06$) and outperformed with very strong evidence the "Linear" and "Circular" models (Body ≠ Linear: BF = 31,897.94, Body ≠ Circular: BF = 4,386.64). For multi-voxel activity patterns, we found that the "Body" model was the best ($r = 0.70 \pm 0.12$), outperformed the "Linear" model with very strong evidence (Body ≠ Linear: BF = 3,938.28) and outperformed with positive evidence the "Circular" model (Body ≠ Circular: BF = 5.66). Finally, for functional connectivity, we found that the "Linear" model was the best ($r = 0.62 \pm 0.20$), outperformed the "Body" model with positive evidence (Linear ≠ Body: BF = 4.67) and outperformed to "Circular" model with very strong evidence (Linear ≠ Circular: BF = 73.00).

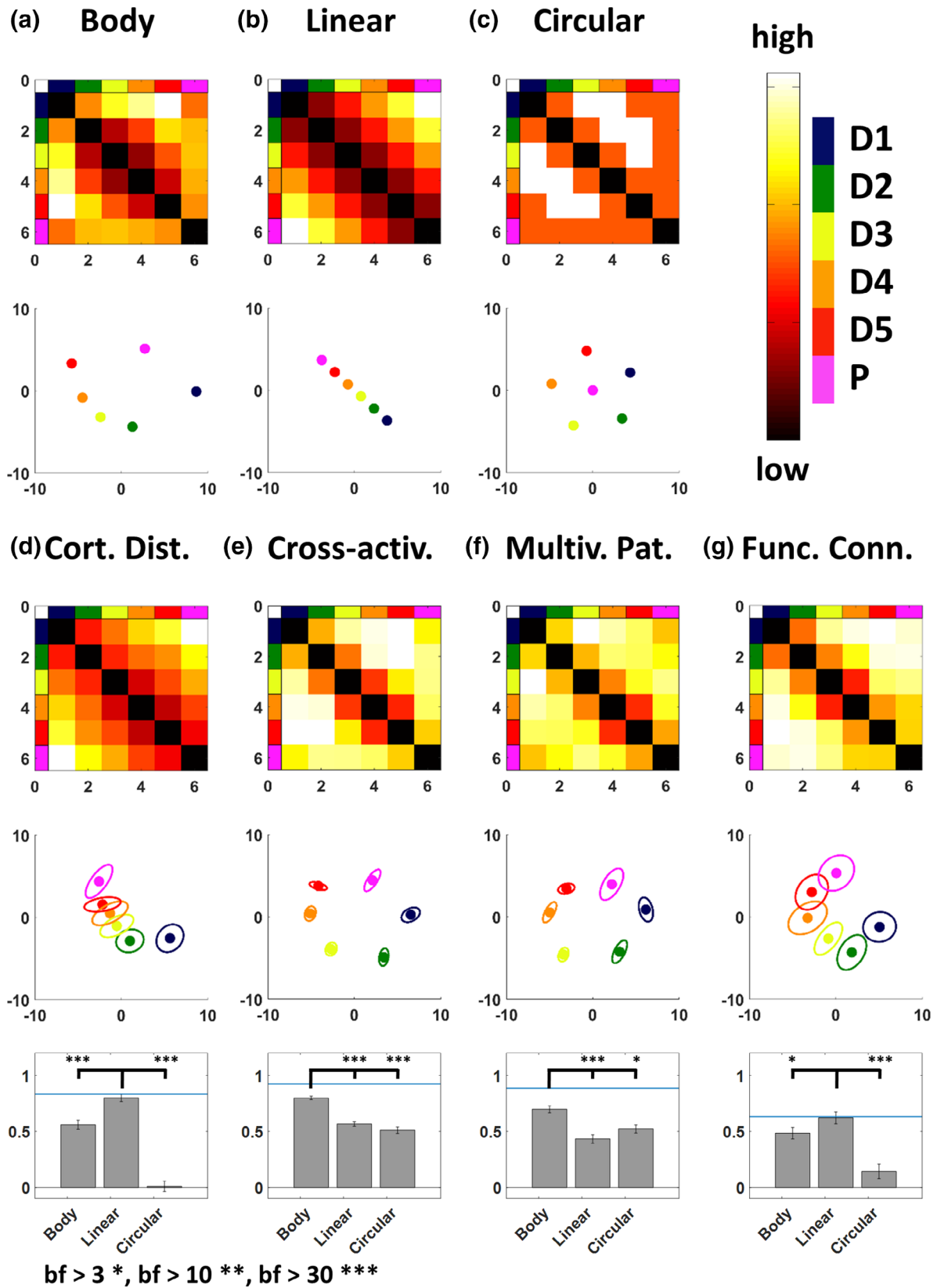**FIGURE 6** Dissimilarity analysis. (a–c) Dissimilarity matrix and 2D configuration for the "Body," "Linear," and "Circular" models. (d–g) Dissimilarity matrix and 2D configuration for the dissimilarity measures based on cortical distances, cross-activations, multi-voxel activity patterns and functional connectivity. The correlations between each dissimilarity measure and the three models are shown in the corresponding bar plots. Asterisks indicate the level of evidence found across Bayesian comparisons. The blue line indicates the noise ceiling. Data presented here are averaged across hands

As a control analysis, to confirm that the aforementioned results cannot be explained by the variance associated with the fingers only, we replicated the whole dissimilarity analysis by excluding the palm from the data, leading to 5x5 dissimilarity matrices across the five fingers. First, we found that the variance explained by the best models was similar when considering the palm and the five fingers or when considering only the five fingers (Figure S6). However, when only considering the five fingers, the analysis could not disambiguate between the "Body" and "Linear" models. Thus, only when considering the palm and the fingers together, it is possible to highlight a double dissociation between dissimilarity measures best matching the models related to the shape of a hand (cross-activations and multi-voxel activity patterns) and dissimilarity measures best matching the model related to somatotopy (cortical distances and functional connectivity).

To summarize, dissimilarity analysis showed that cross-activations and multi-voxel activity patterns were related to the shape of a hand, while cortical distances and functional connectivity were rather related to somatotopy. This shows that the representational geometry of hand activations properties (with the exception of functional connectivity) matched the physical structure of the hand rather than the somatotopic organization of hand representations.

4 | DISCUSSION

The present study aimed at investigating PR in human S1 and its relationship with the five FRs, by analyzing (a) the cortical distances between somatotopic representations (cortical distance), (b) how PR and FRs cross-activate during tactile stimulation (cross-activation), (c) the similarity between activity patterns during tactile stimulation (multi-voxel activity pattern), and (d) how PR and FRs are functionally connected to each other (functional connectivity). During the acquisition of fMRI data at ultra-high field (7T), six hand regions (D1—D2—D3—D4—D5—PALM) on each side of the body were stimulated using natural touch in a group of healthy subjects. This allowed us to identify the tactile representations of the stimulated hand regions within S1. First, we demonstrated the serial arrangement of the somatotopic sequence: D1—D2—D3—D4—D5—PALM. Second, we found that this somatotopic sequence is not reflected in the activation properties of PR and FRs, with the exception of functional connectivity (see below). Instead, the representational geometry of activations within hand representations better matches the physical shape of the hand rather than the somatotopic organization of its representations.

4.1 | Mismatch between S1 hand somatotopy and hand structure in humans

The results obtained from the analysis of cortical distances between PR and FRs confirm that the PRs in human S1 are located medially with respect to the representations of D5, corresponding to a serial somatotopic arrangement in S1 (Blankenburg et al., 2003; Moore et al., 2000; Rasmussen & Penfield, 1947). This layout does not

correspond to the radial distribution of fingers along the palm on the body, thus creating a discontinuity between S1 hand somatotopy and the physical structure of the hand in humans. Discontinuities between somatotopy and body structure have been well documented in primates (Felleman, Nelson, Sur, & Kaas, 1983; Kaas et al., 1979; Merzenich, Kaas, Sur, & Lin, 1978; Nelson, Sur, Felleman, & Kaas, 1980; Rasmussen & Penfield, 1947; Sur, Nelson, & Kaas, 1982). In particular, the latero-medial arrangement of fingers (D1—D2—D3—D4—D5) in S1, which is found in all primates, forms a hand-arm discontinuity with the latero-medial arrangement of the rest of the arm (distal to proximal).

Interestingly, different somatotopic layouts of the pads (i.e., distal palm and base of the fingers) and fingers have been observed in S1 across primate species (Felleman et al., 1983; Merzenich et al., 1978; Nelson et al., 1980; Sur et al., 1982). In Owl and Squirrel Monkeys, the representations of the pads are included in FRs as their most proximal part (Merzenich et al., 1978; Sur et al., 1982). This is also the case in humans (Blankenburg et al., 2003; Sanchez-Panchuelo et al., 2012, 2014; Schweisfurth et al., 2011, 2014). Contrastingly, in Cebus and Macaque Monkeys, the representations of the pads lie medially to D5 (Felleman et al., 1983; Nelson et al., 1980). Thus, the location of the separation forming the somatotopic hand-arm discontinuity appears to vary across primate species. Furthermore, this somatotopic polymorphism does not correspond to phylogenetic relations between primate species (Springer et al., 2012), possibly indicating that a conversion of hand somatotopic layout may have occurred several times during primate evolution. Based on results from this study and previous studies in primates, the proximal part of the palm is represented medially with respect to the five fingers in S1 in all studied primate species (present study and Blankenburg et al., 2003; Felleman et al., 1983; Merzenich et al., 1978; Moore et al., 2000; Nelson et al., 1980; Rasmussen & Penfield, 1947; Sur et al., 1982). Thus, the proximal part of the palm can be considered a reliable landmark in S1 to study somatotopy within and across primate species.

4.2 | Mismatch between S1 hand somatotopy and S1 hand functional organization in humans

Previous studies focusing on fingers reported that S1 cross-activations between FRs followed a pattern compatible with S1 somatotopy, that is, the adjacency between FRs in S1 predicts the degree of cross-activations (Besle et al., 2014; Martuzzi et al., 2014). Similarly, a study focusing on motor representations of fingers showed that multi-voxel activity patterns in S1 associated with finger movements are well described by a somatotopic model of finger adjacency (Ejaz et al., 2015), although these patterns were best described by the natural statistics of hand usage. This suggests that when considering FRs only, a consistency is found between the finger sequence on the hand, the finger somatotopy in S1, and finger activation properties in S1.

Our analyses of PR and FRs activation properties tested whether the S1 palm-to-fingers somatotopy predicts palm-to-fingers functional

coupling, as measured by cross-activations, multi-voxel activity patterns and resting-state functional connectivity. Importantly, considering the natural usage of the palm in synergy with the fingers for hand function, there is no a priori reason to expect stronger coupling between PR and FRs located closer to PR in S1 (e.g., between palm and D5). Concerning resting-state functional connectivity, dissimilarity analysis showed that functional connectivity matched better with the model reflecting S1 somatotopy. This result can be explained by the well-documented influence of cortical distance on resting-state functional connectivity in both topographically and non-topographically organized brain areas (Alexander-Bloch et al., 2013; Ercsey-Ravasz et al., 2013; Raemaekers et al., 2014; Salvador et al., 2005). This suggests a possible confound resulting from the use of resting-state functional connectivity to investigate the relationship between topographic and functional organizations. More interestingly, our statistical analyses of cross-activations and multi-voxel activity patterns revealed that the activation properties of PR and FRs, indeed, do not reflect S1 palm-to-fingers somatotopy. Our analyses of cross-activations highlighted that the palm is coupled most strongly with D1 and D5. Similarly, multi-voxel activity patterns suggested that palm stimulation induced activity patterns most similar to D1 and D5 stimulation. This pattern of activation properties is compatible with the physical shape of the hand where, at rest, the tips of D1 and D5 are closer to the center of the palm compared to other fingers. This view was further supported by dissimilarity analysis showing that the representational geometry of hand representations in S1 matched better with the models reflecting the shape of a hand (except for functional connectivity, see below). Another possibility is that the natural statistics of tactile experience during daily life leads to increased likelihood of palm-D1 and palm-D5 co-stimulation (Ejaz et al., 2015). Whether the observed associations (palm-D1 and palm-D5) are better explained by the statistics of use-related tactile stimulation on the hand rather than simply the physical shape of the hand remains to be investigated. Note, however, that natural statistics of tactile stimulation depends on the hand structure, which would make the two hypotheses complementary.

4.3 | Differences between the right and left hands

Our data also revealed interesting differences between the dominant right hand and the non-dominant left hand in our right-handed participants. We found that the right-hand has overall larger distances between PR and FRs, which might suggest larger cortical territories in S1 for the dominant right hand. However, the inter-digit distances did not differ between right and left hands (Figure S7), thus suggesting that the aforementioned effect is rather due to PR being located further away from FRs. This is in line with previous fMRI reports showing no difference in size between right and left finger representations (Boakye, Huckins, Szeverenyi, Taskey, & Hodge, 2000; Schweisfurth et al., 2018). Second, we found reduced functional connectivity between PR and FRs for the right hand compared to the left hand, which is compatible with the previous finding of larger cortical distances for the right hand, as

increased cortical distance is associated with reduced functional connectivity (Alexander-Bloch et al., 2013; Ercsey-Ravasz et al., 2013; Raemaekers et al., 2014; Salvador et al., 2005). Finally, we also found reduced pattern dissimilarity between PR and FRs for the right hand compared to the left hand, which might reflect the increased usage of the dominant hand for object manipulation (Andersen & Siebner, 2018).

4.4 | Plasticity in topographically organized sensory areas

It is believed that topographically organized cortical sensory maps evolved as an optimal solution for energy-efficient spatio-temporal computations (Kaas, 1997). It is currently accepted that topographic maps are shaped by a combination of at least two different factors. First, during development, the axonal pathways from the skin to the cortex are established through molecular matching interactions, which is governed by genetics (Udin & Fawcett, 1988). The formation of a prototypic topography of sensory maps during development would explain why individuals from a same species share a common architecture. Second, during daily life experience, the spatio-temporal receptive fields of neuronal populations are tuned by sensory stimulation and associated synaptic plasticity (Buonomano & Merzenich, 1998).

Our results provide an important account of mismatch between topographical and functional organizations. This supports the view that functional organization, which is consistent with the peripheral structure of the sensory space, can emerge despite the mismatch between topographical organization and the structure of the sensory space. However, our data could not disambiguate between possible contributions of the structure of the sensory space (i.e., the shape of the hand) and of the natural statistics of tactile stimulation received during everyday life (Ejaz et al., 2015) in shaping the functional organization of hand representations. Nevertheless, these two factors are by definition impossible to disentangle in normal conditions, because the physical structure of the body directly impacts the pattern of natural stimulation during everyday life interactions.

Crucially, topographic maps require the continuous competition and interaction between inputs to maintain a normal organization, which is naturally provided during activities of daily living (Buonomano & Merzenich, 1998). An extreme example of plasticity in adult primary somatosensory areas is observed following limb amputation (Flor et al., 1995; Kaas, Merzenich, & Killackey, 1983; Makin et al., 2013; Makin & Flor, 2020; Serino et al., 2017) or to a lesser extent following limb immobilization (Langer, Hänggi, Müller, Simmen, & Jäncke, 2012; Liepert, Tegenthoff, & Malin, 1995; Zanette et al., 1997). Furthermore, it has been shown that even a brief exposition to repeated sensory stimulation can induce plasticity in primary somatosensory areas (Godde, Spengler, & Dinse, 1996; Muret et al., 2016; Pleger et al., 2001, 2003). Similar observations are found for the visual system and the auditory system (Bilecen et al., 2000; Chino, Kaas, Smith, Langston, & Cheng, 1992; Kaas, 1991; Kaas et al., 1990; Merabet & Pascual-Leone, 2010; Syka, 2002). Considering the results of the present study in light of the capacity of sensory

areas to adapt to changes in the structure of the sensory space, a consistency between somatotopic and functional organizations could be expected. A possible explanation is that a certain degree of flexibility in the consistency between topographic and functional organizations in sensory areas is tolerated. In other words, the metabolic energy cost to tolerate such mismatch is lower than the energy cost required for reorganization. This might suggest that processing mismatched sensory inputs would lead to reorganization only in case of substantial inconsistency.

4.5 | Study limitations

We provided tactile stimulation by means of manual stroking delivered by a human experimenter, thus introducing inherent variability in the timing, intensity and extent of stimulation. This choice was motivated by previous work from our group, showing that natural touch is able to induce reliable activations in S1 (Akselrod et al., 2017; Martuzzi et al., 2014; Serino et al., 2017), and stronger activations compared to mechanical stimulation (van der Zwaag et al., 2015). Although the increased variability associated with natural touch might contribute to the increased signal quality, the lack of controllability might have introduced systematic biases towards a specific body part. Thus, we cannot exclude that at least part of the variance explained by our results might be attributed to the lack of controllability of natural touch. In addition, we used a fixed order of stimulation rather than randomized, thus we cannot entirely rule out the possibility of a temporal confound affecting our data. However, we conducted control analyses to test whether the effect predicted by the temporal confound could explain part of the variance in our data and found no evidence supporting a potential confound of the temporal order (Table S3–S6 and Figure S8). Finally, in the present study, we considered S1 as a single functional unit. However, it is known that multiple tactile representations are located within subregions of S1 (e.g., Kaas et al., 1979). Investigating the multiple representations within S1 requires dedicated protocols to efficiently identify the separate homologous representations of the same hand region (see Sanchez-Panchuelo et al., 2012), which was not possible with the present data. Future studies using dedicated protocols might investigate the different subregions of S1 to assess whether the present findings generalize across all S1 subregions.

5 | CONCLUSIONS

The present study characterizes the properties of PR and its relationship with FRs in human S1. In particular, we investigated the relationship between somatotopic and functional organizations of hand representations and reported a mismatch between the two with respect to palm-finger activation properties. To further study the link between functional properties of tactile hand representations, physical structure of the hand and natural statistics of tactile stimulation, fMRI mapping data (as in the present study) should be combined with behavioral data (e.g., hand tracking during object manipulation). This would allow investigating inter-individual differences in tactile perception and motor skills and would allow studying brain–body plasticity in clinical conditions like amputation or stroke.

CONFLICT OF INTEREST

None of the authors has competing interests.

DATA AVAILABILITY STATEMENT

The processed data presented in the Results section (cortical distances, cross-activations, multi-voxel patterns, resting-state functional connectivity and dissimilarity analysis) are openly available on the Zenodo platform (Akselrod, Martuzzi, van der Zwaag, Blanke, & Serino, 2021). Data analyses were carried out using publicly available resources and/or are fully reproducible from the information provided in the Methods section. Raw data will not be shared to guarantee privacy and confidentiality for the participants.

ORCID

Michel Akselrod 🄳 https://orcid.org/0000-0002-0805-7955

REFERENCES

Akselrod, M., Martuzzi, R., Serino, A., van der Zwaag, W., Gassert, R., & Blanke, O. (2017). Anatomical and functional properties of the foot and leg representation in areas 3b, 1 and 2 of primary somatosensory cortex in humans: A 7T fMRI study. *NeuroImage*, *159*, 473–487. https://doi.org/10.1016/j.neuroimage.2017.06.021

Akselrod, M., Martuzzi, R., van der Zwaag, W., Blanke, O., & Serino, A. (2021). Open Dataset - Relation between palm and finger cortical representations in primary somatosensory cortex: A 7T fMRI study. *Zenodo*, https://doi.org/10.5281/zenodo.4017495

Alexander-Bloch, A. F., Vértes, P. E., Stidd, R., Lalonde, F., Clasen, L., Rapoport, J., ... Gogtay, N. (2013). The anatomical distance of functional connections predicts brain network topology in health and schizophrenia. *Cerebral Cortex*, *23*, 127–138. https://doi.org/10.1093/cercor/bhr388

Andersen, K. W., & Siebner, H. R. (2018). Mapping dexterity and handedness: Recent insights and future challenges. *Current Opinion in Behavioral Sciences*, *20*, 123–129. https://doi.org/10.1016/j.cobeha.2017.12.020

Besle, J., Sánchez-Panchuelo, R. M., Bowtell, R., Francis, S., & Schluppeck, D. (2014). Event-related fMRI at 7T reveals overlapping cortical representations for adjacent fingertips in S1 of individual subjects. *Human Brain Mapping*, *35*, 2027–2043. https://doi.org/10.1002/hbm.22310

Bilecen, D., Seifritz, E., Radu, E. W., Schmid, N., Wetzel, S., Probst, R., & Scheffler, K. (2000). Cortical reorganization after acute unilateral hearing loss traced by fMRI. *Neurology*, *54*, 765–767. https://doi.org/10.1212/WNL.54.3.765

Blankenburg, F., Ruben, J., Meyer, R., Schwiemann, J., & Villringer, A. (2003). Evidence for a rostral-to-caudal somatotopic organization in human primary somatosensory cortex with mirror-reversal in areas 3b and 1. *Cerebral Cortex*, *13*, 987–993. https://doi.org/10.1093/cercor/13.9.987

Boakye, M., Huckins, S. C., Szeverenyi, N. M., Taskey, B. I., & Hodge, C. J. (2000). Functional magnetic resonance imaging of somatosensory cortex activity produced by electrical stimulation of the median nerve or tactile stimulation of the index finger. *Journal of Neurosurgery*, *93*, 774–783. https://doi.org/10.3171/jns.2000.93.5.0774

Bullock, I. M., & Dollar, A. M. (2011). Classifying human manipulation behavior. *IEEE International Conference on Rehabilitation Robotics*. https://doi.org/10.1109/ICORR.2011.5975408

Buonomano, D. V., & Merzenich, M. M. (1998). CORTICAL PLASTICITY: From synapses to maps. *Annual Review of Neuroscience*, *21*, 149–186. https://doi.org/10.1146/annurev.neuro.21.1.149

Chino, Y. M., Kaas, J. H., Smith, E. L., Langston, A. L., & Cheng, H. (1992). Rapid reorganization of cortical maps in adult cats following restricted deafferentation in retina. *Vision Research*, *32*, 789–796. https://doi.org/10.1016/0042-6989(92)90021-A

Cooper, M., & Seber, G. A. F. (1985). Multivariate observations. *Journal of Marketing Research*, *22*, 226. https://doi.org/10.2307/3151376

Desikan, R. S., Segonne, F., Fischl, B., Quinn, B. T., Dickerson, B. C., Blacker, D., … Killiany, R. J. (2006). An automated labeling system for subdividing the human cerebral cortex on MRI scans into gyral based regions of interest. *NeuroImage*, *31*, 968–980.

Ejaz, N., Hamada, M., & Diedrichsen, J. (2015). Hand use predicts the structure of representations in sensorimotor cortex. *Nature Neuroscience*, *103*, 1–10. https://doi.org/10.1038/nn.4038

Ercsey-Ravasz, M., Markov, N. T., Lamy, C., VanEssen, D. C., Knoblauch, K., Toroczkai, Z., & Kennedy, H. (2013). A predictive network model of cerebral cortical connectivity based on a distance rule. *Neuron*, *80*, 184–197. https://doi.org/10.1016/j.neuron.2013.07.036

Felleman, D. J., Nelson, R. J., Sur, M., & Kaas, J. H. (1983). Representations of the body surface in areas 3b and 1 of postcentral parietal cortex of cebus monkeys. *Brain Research*, *268*, 15–26. https://doi.org/10.1016/0006-8993(83)90386-4

Fisher, R. A. (1915). Frequency distribution of the values of the correlation coefficient in samples from an indefinitely large population. *Biometrika*, *10*, 507. https://doi.org/10.2307/2331838

Flor, H., Elbert, T., Knecht, S., Wienbruch, C., Pantev, C., Birbaumers, N., … Taub, E. (1995). Phantom-limb pain as a perceptual correlate of cortical reorganization following arm ampFlor, H. et al. (1995). Phantom-limb pain as a perceptual correlate of cortical reorganization following arm amputation. *Letters to Nature*, *375*, 482–484.

Glover, G. H., Li, T. Q., & Ress, D. (2000). Image-based method for retrospective correction of physiological motion effects in fMRI: RETROICOR. *Magnetic Resonance in Medicine*, *44*, 162–167. https://doi.org/10.1002/1522-2594(200007)44:1<162::AID-MRM23>3.0.CO;2-E

Godde, B., Spengler, F., & Dinse, H. (1996). Associative pairing of tactile stimulation induces somatosensory cortical reorganization in rats and humans. *Neuroreport*, *8*, 281–285.

Hashimoto, I., Mashiko, T., Kimura, T., & Imada, T. (1999). Are there discrete distal-proximal representations of the index finger and palm in the human somatosensory cortex? A neuromagnetic study. *Clinical Neurophysiology*, *110*, 430–437. https://doi.org/10.1016/S1388-2457(98)00018-2

Hoijtink, H., Mulder, J., van Lissa, C., Gu, X., 2019. A tutorial on testing hypotheses using the Bayes factor. *Psychological Methods* https://doi.org/10.1037/met0000201, *24*, 539, 556

Kaas, J. H. (1991). Plasticity of sensory and motor maps in adult mammals. *Annual Review of Neuroscience*, *14*, 137–167. https://doi.org/10.1146/annurev.neuro.14.1.137

Kaas, J. H. (1997). Topographic maps are fundamental to sensory processing. *Brain Research Bulletin*, *44*, 107–112. https://doi.org/10.1016/S0361-9230(97)00094-4

Kaas, J. H., Krubitzer, L. A., Chino, Y. M., Langston, A. L., Polley, E. H., & Blair, N. (1990). Reorganization of retinotopic cortical maps in adult mammals after lesions of the retina. *Science*, *248*(4952), 229–231. https://doi.org/10.1126/science.2326637

Kaas, J. H., Merzenich, M. M., & Killackey, H. P. (1983). The reorganization of somatosensory cortex following peripheral nerve damage in adult and developing mammals. *Annual Review of Neuroscience*, *6*, 325–356. https://doi.org/10.1146/annurev.ne.06.030183.001545

Kaas, J. H., Nelson, R. J., Sur, M., Lin, C. S., & Merzenich, M. M. (1979). Multiple representations of the body within the primary somatosensory cortex of primates. *Science*, *204*, 521–523. https://doi.org/10.1126/science.107591

Kass, R. E., & Raftery, A. E. (1995). Bayes factors. *Journal of the American Statistical Association*, *90*, 773–795. https://doi.org/10.1080/01621459.1995.10476572

Kriegeskorte, N., Mur, M., & Bandettini, P. (2008). Representational similarity analysis - connecting the branches of systems neuroscience. *Frontiers in Systems Neuroscience*, *2*, 4. https://doi.org/10.3389/neuro.06.004.2008

Langer, N., Hänggi, J., Müller, N. A., Simmen, H. P., & Jäncke, L. (2012). Effects of limb immobilization on brain plasticity. *Neurology*, *78*, 182–188. https://doi.org/10.1212/WNL.0b013e31823fcd9c

Liepert, J., Tegenthoff, M., & Malin, J. P. (1995). Changes of cortical motor area size during immobilization. *Electroencephalography and Clinical Neurophysiology: Electromyography*, *97*, 382–386. https://doi.org/10.1016/0924-980X(95)00194-P

Makin, T. R., Cramer, A. O., Scholz, J., Hahamy, A., Slater, D. H., Tracey, I., & Johansen-Berg, H. (2013). Deprivation-related and use-dependent plasticity go hand in hand. *Elife*, *2*, 1–15. https://doi.org/10.7554/eLife.01273

Makin, T. R., & Flor, H. (2020). Brain (re)organisation following amputation: Implications for phantom limb pain. *NeuroImage*, *218*, 116943. https://doi.org/10.1016/j.neuroimage.2020.116943

Marques, J. P., Kober, T., Krueger, G., van der Zwaag, W., Van de Moortele, P. F., & Gruetter, R. (2010). MP2RAGE, a self bias-field corrected sequence for improved segmentation and T1-mapping at high field. *NeuroImage*, *49*, 1271–1281. https://doi.org/10.1016/j.neuroimage.2009.10.002

Martuzzi, R., van der Zwaag, W., Dieguez, S., Serino, A., Gruetter, R., & Blanke, O. (2015). Distinct contributions of Brodmann areas 1 and 2 to body ownership. *Social Cognitive and Affective Neuroscience*, *10*, 1449–1459. https://doi.org/10.1093/scan/nsv03

Martuzzi, R., van der Zwaag, W., Farthouat, J., Gruetter, R., & Blanke, O. (2014). Human finger somatotopy in areas 3b, 1, and 2: A 7T fMRI study using a natural stimulus. *Human Brain Mapping*, *35*, 213–226. https://doi.org/10.1002/hbm.22172

Mehring, C., Akselrod, M., Bashford, L., Mace, M., Choi, H., Blüher, M., … Burdet, E. (2019). Augmented manipulation ability in humans with six-fingered hands. *Nature Communications*, *10*, 2401. https://doi.org/10.1038/s41467-019-10306-w

Merabet, L. B., & Pascual-Leone, A. (2010). Neural reorganization following sensory loss: The opportunity of change. *Nature Reviews. Neuroscience*, *11*, 44–52. https://doi.org/10.1038/nrn2758

Merzenich, M. M., Kaas, J. H., Sur, M., & Lin, C. S. (1978). Double representation of the body surface within cytoarchitectonic areas 3b and 1 in "SI" in the owl monkey (*Aotus trivirgatus*). *The Journal of Comparative Neurology*, *181*, 41–73. https://doi.org/10.1002/cne.901810104

Moore, C. I., Stern, C. E., Corkin, S., Fischl, B., Gray, A. C., Rosen, B. R., & Dale, A. M. (2000). Segregation of Somatosensory Activation in the Human Rolandic Cortex Using fMRI. *Journal of Neurophysiology*, *84*, 558–569.

Muret, D., Daligault, S., Dinse, H. R., Delpuech, C., Mattout, J., Reilly, K. T., & Farne, A. (2016). Neuromagnetic correlates of adaptive plasticity across the hand-face border in human primary somatosensory cortex. *Journal of Neurophysiology*, *115*, 2095–2104. https://doi.org/10.1152/jn.00628.2015

Nelson, R. J., Sur, M., Felleman, D. J., & Kaas, J. H. (1980). Representations of the body surface in postcentral parietal cortex of *Macaca fascicularis*. *The Journal of Comparative Neurology*, 192, 611–643. https://doi.org/10.1002/cne.901920402

Nili, H., Wingfield, C., Walther, A., Su, L., Marslen-Wilson, W., & Kriegeskorte, N. (2014). A toolbox for representational similarity analysis. *PLoS Computational Biology*, 10, e1003553. https://doi.org/10.1371/journal.pcbi.1003553

Oldfield, R. C. (1971). The assessment and analysis of handedness: The Edinburgh inventory. *Neuropsychologia*, 9, 97–113. https://doi.org/10.1016/0028-3932(71)90067-4

Olman, C. A., Van de Moortele, P. F., Schumacher, J. F., Guy, J. R., Uğurbil, K., & Yacoub, E. (2010). Retinotopic mapping with spin echo BOLD at 7T. *Magnetic Resonance Imaging*, 28, 1258–1269. https://doi.org/10.1016/j.mri.2010.06.001

Pleger, B., Dinse, H. R., Ragert, P., Schwenkreis, P., Malin, J. P., & Tegenthoff, M. (2001). Shifts in cortical representations predict human discrimination improvement. *Proceedings of the National Academy of Sciences of the United States of America*, 98, 12255–12260. https://doi.org/10.1073/pnas.191176298

Pleger, B., Foerster, A. F., Ragert, P., Dinse, H. R., Schwenkreis, P., Malin, J. P., ... Tegenthoff, M. (2003). Functional imaging of perceptual learning in human primary and secondary somatosensory cortex. *Neuron*, 40, 643–653. https://doi.org/10.1016/S0896-6273(03)00677-9

Pont, K., Wallen, M., & Bundy, A. (2009). Conceptualising a modified system for classification of in-hand manipulation. *Australian Occupational Therapy Journal*, 56, 2–15. https://doi.org/10.1111/j.1440-1630.2008.00774.x

Raemaekers, M., Schellekens, W., van Wezel, R. J. A., Petridou, N., Kristo, G., & Ramsey, N. F. (2014). Patterns of resting state connectivity in human primary visual cortical areas: A 7T fMRI study. *NeuroImage*, 84, 911–921. https://doi.org/10.1016/j.neuroimage.2013.09.060

Rasmussen, T., & Penfield, W. (1947). Further studies of the sensory and motor cerebral cortex of man. *Federation Proceedings*, 6, 452–460.

Saadon-Grosman, N., Tal, Z., Itshayek, E., Amedi, A., & Arzy, S. (2015). Discontinuity of cortical gradients reflects sensory impairment. *Proceedings of the National Academy of Sciences*, 112, 16024–16029. https://doi.org/10.1073/pnas.1506214112

Salomon, R., Darulova, J., Narsude, M., & Van Der Zwaag, W. (2014). Comparison of an 8-hannel and a 32-channel coil for high-resolution fMRI at 7 T. *Brain Topography*, 27, 209–212. https://doi.org/10.1007/s10548-013-0298-6

Salvador, R., Suckling, J., Coleman, M. R., Pickard, J. D., Menon, D., & Bullmore, E. (2005). Neurophysiological architecture of functional magnetic resonance images of human brain. *Cerebral Cortex*, 15, 1332–2342. https://doi.org/10.1093/cercor/bhi016

Sanchez-Panchuelo, R. M., Besle, J., Beckett, A., Bowtell, R., Schluppeck, D., & Francis, S. (2012). Within-digit functional parcellation of Brodmann areas of the human primary somatosensory cortex using functional magnetic resonance imaging at 7 tesla. *The Journal of Neuroscience*, 32, 15815–15822. https://doi.org/10.1523/jneurosci.2501-12.2012

Sanchez-Panchuelo, R. M., Besle, J., Mougin, O., Gowland, P., Bowtell, R., Schluppeck, D., & Francis, S. (2014). Regional structural differences across functionally parcellated Brodmann areas of human primary somatosensory cortex. *NeuroImage*, 93, 221–230. https://doi.org/10.1016/j.neuroimage.2013.03.044

Sanchez-Panchuelo, R. M., Francis, S., Bowtell, R., & Schluppeck, D. (2010). Mapping human somatosensory cortex in individual subjects with 7T functional MRI. *Journal of Neurophysiology*, 103, 2544–2556. https://doi.org/10.1152/jn.01017.2009

Sawilowsky, S. S. (2009). New effect size rules of thumb. *Journal of Modern Applied Statistical Methods*, 8, 597–599. https://doi.org/10.22237/jmasm/1257035100

Schweisfurth, M. a., Frahm, J., & Schweizer, R. (2014). Individual fMRI maps of all phalanges and digit bases of all fingers in human primary somatosensory cortex. *Frontiers in Human Neuroscience*, 8, 658. https://doi.org/10.3389/fnhum.2014.00658

Schweisfurth, M. A., Frahm, J., Farina, D., & Schweizer, R. (2018). Comparison of fMRI digit representations of the dominant and non-dominant hand in the human primary somatosensory cortex. *Frontiers in Human Neuroscience*, 12. https://doi.org/10.3389/fnhum.2018.00492

Schweisfurth, M. A., Schweizer, R., & Frahm, J. (2011). Functional MRI indicates consistent intra-digit topographic maps in the little but not the index finger within the human primary somatosensory cortex. *NeuroImage*, 56, 2138–2143. https://doi.org/10.1016/j.neuroimage.2011.03.038

Schweizer, R., Voit, D., & Frahm, J. (2008). Finger representations in human primary somatosensory cortex as revealed by high-resolution functional MRI of tactile stimulation. *NeuroImage*, 42, 28–35. https://doi.org/10.1016/j.neuroimage.2008.04.184

Serino, A., Akselrod, M., Salomon, R., Martuzzi, R., Blefari, M. L., Canzoneri, E., ... Blanke, O. (2017). Upper limb cortical maps in amputees with targeted muscle and sensory reinnervation. *Brain*, 140, 2993–3011. https://doi.org/10.1093/brain/awx242

Speck, O., Stadler, J., & Zaitsev, M. (2008). High resolution single-shot EPI at 7T. *Magnetic Resonance Materials in Physics, Biology and Medicine*, 21, 73–86. https://doi.org/10.1007/s10334-007-0087-x

Springer, M. S., Meredith, R. W., Gatesy, J., Emerling, C. A., Park, J., Rabosky, D. L., ... Murphy, W. J. (2012). Macroevolutionary dynamics and historical biogeography of primate diversification inferred from a species supermatrix. *PLoS One*, 7, e49521. https://doi.org/10.1371/journal.pone.0049521

Stringer, E. A., Chen, L. M., Friedman, R. M., Gatenby, C., & Gore, J. C. (2011). Differentiation of somatosensory cortices by high-resolution fMRI at 7T. *NeuroImage*, 54, 1012–1020. https://doi.org/10.1016/j.neuroimage.2010.09.058

Stringer, E. A., Qiao, P. G., Friedman, R. M., Holroyd, L., Newton, A. T., Gore, J. C., & Chen, L. M. (2014). Distinct fine-scale fMRI activation patterns of contra- and ipsilateral somatosensory areas 3b and 1 in humans. *Human Brain Mapping*, 35, 4841–4857. https://doi.org/10.1002/hbm.22517

Sur, M., Nelson, R. J., & Kaas, J. H. (1982). Representations of the body surface in cortical areas 3b and 1 of squirrel monkeys: Comparisons with other primates. *The Journal of Comparative Neurology*, 211, 177–192. https://doi.org/10.1002/cne.902110207

Syka, J. (2002). Plastic changes in the central auditory system after hearing loss, restoration of function, and during learning. *Physiological Reviews*, 82, 601–636. https://doi.org/10.1152/physrev.00002.2002

Tourbier, S., Aleman-Gomez, Y., Griffa, A., Bach Cuadra, M., & Hagmann, P. (2020). connectomicslab/connectomemapper3: Connectome Mapper v3.0.0-beta-RC2 (Version v3.0.0-beta-RC2). Zenodo. http://doi.org/10.5281/zenodo.3475969.

Udin, S. B., & Fawcett, J. W. (1988). Formation of topographic maps. *Annual Review of Neuroscience*, 11, 289–327. https://doi.org/10.1146/annurev.ne.11.030188.001445

Van Der Zwaag, W., Gruetter, R., & Martuzzi, R. (2015). Stroking or buzzing? A comparison of somatosensory touch stimuli using 7 tesla fMRI. *PLoS One*, 10, e0134610. https://doi.org/10.1371/journal.pone.0134610

van Ooyen, A., Carnell, A., De Ridder, S., Tarigan, B., Mansvelder, H. D., Bijma, F., ... van Pelt, J. (2014). Independently outgrowing neurons and geometry-based synapse formation produce networks with realistic synaptic connectivity. *PLoS One*, 9, e85858. https://doi.org/10.1371/journal.pone.0085858

van Pelt, J., & van Ooyen, A. (2013). Estimating neuronal connectivity from axonal and dendritic density fields. *Frontiers in Computational Neuroscience*, 7. https://doi.org/10.3389/fncom.2013.00160

Whitfield-Gabrieli, S., & Nieto-Castanon, A. (2012). Conn: A functional connectivity toolbox for correlated and anticorrelated brain networks.

Brain Connectivity, *2*, 125–141. https://doi.org/10.1089/brain.2012.0073

Zanette, G., Tinazzi, M., Bonato, C., Di Summa, A., Manganotti, P., Polo, A., Fiaschi, A. (1997). Reversible changes of motor cortical outputs following immobilization of the upper limb. *Electroencephalography and Clinical Neurophysiology: Electromyography and Motor Control*, *105*, 269–279. https://doi.org/10.1016/S0924-980X(97)00024-6

Zeharia, N., Hertz, U., Flash, T., & Amedi, A. (2015). New whole - body sensory - motor gradients revealed using phase - locked analysis and verified using multivoxel pattern analysis and functional connectivity. *The Journal of Neuroscience*, *35*, 2845–2859. https://doi.org/10.1523/JNEUROSCI.4246-14.2015

SUPPORTING INFORMATION

Additional supporting information may be found online in the Supporting Information section at the end of this article.